Numerical and Literal Aeroelastic-Vehicle-Model Reduction for Feedback Control Synthesis

Brett Newman* and David K. Schmidt†
Arizona State University, Tempe, Arizona 85287

The simplification of a high-order, literal model for large flexible aircraft is discussed. Areas of model fidelity that are critical if the model is to be used for control law synthesis are presented. Several simplification techniques, some new and some widely available, that can deliver the necessary model fidelity are presented and applied to a model from the literature. The techniques include both numerical and analytical approaches. An analytical approach, based on first-order sensitivity theory, is shown to lead not only to excellent numerical results, but also to closed-form analytical expressions for key system dynamic properties such as the pole/zero factors of the vehicle transfer-function matrix. The analytical results are expressed in terms of vehicle vibrational characteristics and rigid-body and aeroelastic stability derivatives, thus providing insight into the underlying causes for critical dynamic characteristics.

Introduction

TO simplify the dynamic analysis and control synthesis, or to ease computational burden in simulation, simple low-order models of the vehicle dynamics are sought. These models, however, must possess the requisite validity in modeling the vehicle characteristics significant in the application. If the model will be used in the synthesis of a feedback system, characteristics critical in a feedback system must be well modeled. This is the first goal of this work, and techniques capable of delivering valid models for multivariable control synthesis will be presented.

A second goal is related to the fact that the physics of the vehicle must be well understood, and models that expose the underlining physical causes for critical dynamic characteristics of the vehicle are desired. This is especially significant in light of the fact that many model reduction procedures in the literature rely on numerical techniques and/or transformations that lead to a model in a form such that the physics of the system are far from transparent in the new model structure. Approximate literal expressions for the factored transfer functions are presented herein that aid in understanding the physics of aeroelastic vehicles and yet constitute model simplifications as well.

Modeling for Dynamic Analysis and Control Synthesis

To accomplish the second goal, a literal model for the vehicle must be available, and the development of such was the subject of Ref. 1. From the nonlinear, literal, time-domain model of an elastic aircraft, the linearized small perturbation longitudinal dynamic equations were developed in the reference. Transformation to the frequency domain leads to the elastic aircraft model in polynomial matrix form[2] given in Appendix A, where elevator deflection δ_E and canard deflection δ_C are the assumed inputs (for a specific configuration example to follow). Typically, vertical acceleration a_z' and pitch rate q' at some location along the fuselage axis are measured responses of interest yielding two additional response equations. This model governs the small perturbation dynamics of the rigid-body degrees of freedom consisting of forward speed u, angle of attack α, pitch angle θ, and pitch rate q, and the generalized elastic degrees of freedom η_i, corresponding to the ith elastic mode in the model. Parameters of interest appearing in Appendix A are trim velocity V_T, a_z' and q' sensor location relative to the vehicle center of mass x, stability derivatives X_i, Z_i, M_i, and F_{ij}, elastic mode vibration frequencies ω_i and damping ratios ζ_i, and elastic mode shapes $\phi_i(x)$ and mode slopes $\phi_i'(x)$ at the sensor location.

Numerical values for the parameters in Appendix A are also available for the vehicle studied in Ref. 1. This is a large supersonic aircraft of reasonably conventional geometry with a low aspect ratio swept wing, conventional tail, and canard (i.e., similar in geometry to the B-1B but much more flexible). The numerical model contains four free-free elastic modes (resulting in a 12th-order model), and the a_z' and q' sensor location corresponds to that of the cockpit. The in vacuo vibration frequencies are 6.3, 7.0, 10.6, and 11.0 rad/s (from Ref. 1) and are considered representative for a large supersonic/hypersonic cruise vehicle with considerable flexibility. The reference flight condition taken here is at Mach 0.6 and altitude 5000 ft. By inclusion of only the first four elastic modes of the structure, a model simplification has already occurred, the implication of which will be discussed next.

Now consider a generic feedback configuration illustrated in Fig. 1, representing the flight and/or structural-mode-control loops, for example. It consists of the interconnected plant (vehicle) matrix $G'(s) = G(s) + \Delta G(s)$ and controller matrix $K(s)$, with excitations from commands Y_c, and responses Y. All signals are multivariable, in general, and $G'(s)$ and $K(s)$ are transfer function matrices.

Of paramount importance in control design is that any simplified model $G(s)$ used in the analysis and synthesis accurately reflects the stability robustness of the true closed-loop system, where stability robustness here refers to the system's

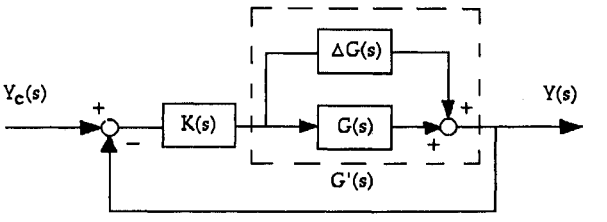

Fig. 1 Generic feedback configuration.

Received May 9, 1989; revision received Aug. 1, 1990; accepted for publication Aug. 9, 1990.

*Research Associate, Aerospace Research Center; currently Doctoral Student, School of Aeronautics and Astronautics, Purdue University, West Lafayette, IN. Student Member AIAA.

†Professor of Engineering and Acting Director, Aerospace Research Center. Associate Fellow AIAA.

ability to maintain stability in the face of loop uncertainties.[3] The genesis of this uncertainty could be due to parameter variations or unmodeled dynamics in G and due to modeling simplification, specifically.

Stability of the true closed-loop system is determined by the zeros of the (true) return difference matrix determinant

$$\det (I + GK + \Delta GK) = 0$$

Assuming the nominal closed-loop system (GK) is stable and the forward-loop perturbation ΔG is stable, the true closed-loop system is stable if

$$\det (I + GK + \epsilon \Delta GK)|_{s=j\omega} \neq 0$$

for all ω and all ϵ, $0 \leq \epsilon \leq 1$, or, equivalently, if $[I + GK(j\omega) + \epsilon \Delta GK(j\omega)]$ remains nonsingular for all ω and all ϵ, $0 \leq \epsilon \leq 1$.

It can be shown[3] that a sufficient condition to guarantee the above inequality is to require

$$\bar{\sigma}[\Delta GK(j\omega)] < \underline{\sigma}[I + GK(j\omega)]$$

for all ω. Here $\underline{\sigma}$ and $\bar{\sigma}$ denote the minimum and maximum singular values of a matrix, respectively. Therefore, the key frequency ranges where stability robustness is potentially a problem is where

$$\bar{\sigma}[\Delta GK(j\omega)] \approx \underline{\sigma}[I + GK(j\omega)] \tag{1}$$

over the (physically) possible ΔGK.

For single-input, single-output systems, Eq. (1) is easily interpreted on a Nyquist diagram. The right side of Eq. (1) corresponds to the distance between a point on the nominal Nyquist contour $GK(j\omega)$ and the critical point at -1. The left side of Eq. (1) corresponds to the distance between the above point on the nominal Nyquist contour and the corresponding point on the perturbed Nyquist contour, $G'K(j\omega)$. Regions where these two distances are approximately equal define the key frequency ranges. The concept generalizes to multi-input, multi-output systems, and, therefore, Eq. (1) defines the only frequency ranges where stability robustness is potentially a problem and certain frequency ranges are more critical than others.

One frequency range pinpointed by Eq. (1) is of course the crossover frequency [i.e., the frequency range where $\underline{\sigma}(GK) \approx \bar{\sigma}(GK) \approx 1$] where relatively small variations in the loop GK can be destabilizing. Moreover, it also includes frequencies where small changes in G can create large ΔGK satisfying Eq. (1) (e.g., systems with near pole-zero cancellations within G in the vicinity of the $j\omega$ axis).

Introduction of any simplified plant model into the loop alters the loop shape (e.g., open-loop Bode) from the true loop shape. If a desirable[3] loop shape is still achieved, however, deviations from the true loop shape may occur in the high- and low-frequency ranges and not significantly affect the results of the design. At low frequencies, adequate loop gain (in GK) is all that is required for acceptable command following/disturbance rejection. In the high-frequency range, the loop gain (in GK) must have adequate rolloff for acceptable noise attenuation. Consequently, an extremely accurate approximation of the true system (G') is frequently not required in either the low- or high-frequency range as long as these two criteria are met. This again leaves the midfrequency range or crossover region as the critical region that must be accurately approximated by any simplified model. In summary, the primary modeling requirement imposed by feedback synthesis applications is to achieve an accurate approximation for the frequency response of the plant in the range of loop gain crossover if the loop gain is large above this frequency range and the loop gain is small below this range. Clearly, the control law $K(s)$ affects these loop gains and determines the crossover range.

A measure of how well a simplified plant model $G(s)$ approximates the true plant model $G'(s)$ over the crossover frequency range ($\omega_1 < \omega < \omega_2$) is the element by element frequency response error. Let the frequency response error matrix be defined by

$$E(j\omega) = G'(j\omega) - G(j\omega) \tag{2}$$

Each i-j element in $E(j\omega)$ describes the frequency response error associated with the corresponding element in $G'(j\omega)$. For $G(s)$ to accurately approximate $G'(s)$ over the crossover frequency range, each element of $E(j\omega)$ and $G'(j\omega)$ must satisfy $|E_{ij}(j\omega)| \ll |G'_{ij}(j\omega)|$ for all ω, $\omega_1 < \omega < \omega_2$. This can be visualized graphically by superimposing the frequency responses of each element of $G'(s)$ and $G(s)$ and noting the differences between the two.

A matrix norm defined by the maximum singular value of the matrix $E(j\omega)$ may also be used to provide a measure of smallness for the error $E(j\omega)$. Recall that the maximum singular value of E is defined as

$$\bar{\sigma}(E) = \bar{\lambda}^{1/2}(EE^*)$$

where $\bar{\lambda}$ denotes the maximum eigenvalue. It can be shown[4] that this norm bounds the magnitude of each element in $E(j\omega)$, i.e., $|E_{ij}(j\omega)| \leq \bar{\sigma}[E(j\omega)]$.

Let the largest value of $\bar{\sigma}[E(j\omega)]$ over the crossover frequency range define a crossover frequency norm

$$\|E(j\omega)\|_{cf} = \max_{\omega_1 < \omega < \omega_2} \bar{\sigma}[E(j\omega)] \tag{3}$$

and the value of this norm may be taken as a relevant measure of closeness between the true and approximate model. Note that using the ∞ norm, or

$$\|E(j\omega)\|_{\infty} = \max_{0 < \omega < \infty} \bar{\sigma}[E(j\omega)]$$

would be far too conservative for our purposes here.

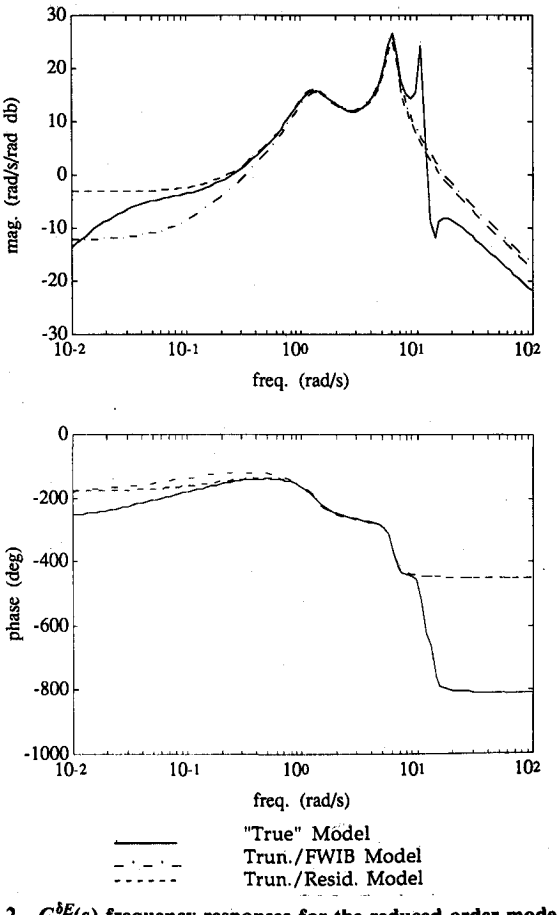

Fig. 2 $G_{q'}^{\delta E}(s)$ frequency responses for the reduced order models.

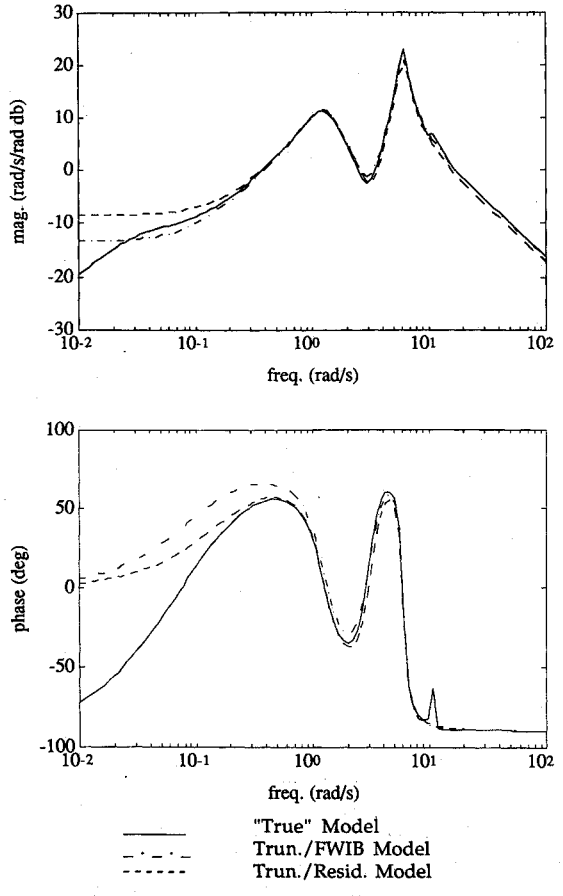

Fig. 3 $G_q^{\delta C}(s)$ **frequency responses for the reduced order models.**

Order Reduction and Simplification

Some order reduction techniques that can lead to good approximations meeting the criteria that were just mentioned will now be highlighted.

Frequency-Weighted Internally Balanced Reduction[5]

Assume the system in Appendix A is described in state-space form, or

$$\dot{x} = Ax + Bu \tag{4a}$$

$$y = Cx + Du \tag{4b}$$

Two frequency-dependent matrices of interest are

$$X(j\omega) = (j\omega I - A)^{-1}B$$

$$Y(j\omega) = C(j\omega I - A)^{-1}$$

$X(j\omega)$ reflects the system's input behavior since each column is the state vector's frequency response associated with the related input, whereas $Y(j\omega)$ reflects the system's output behavior because each column is the output frequency response associated with the related state. The controllability and observability grammians are related to $X(j\omega)$ and $Y(j\omega)$ by

$$X = \frac{1}{2\pi}\int_{-\infty}^{\infty} X(j\omega)X^T(-j\omega)\,d\omega$$

$$Y = \frac{1}{2\pi}\int_{-\infty}^{\infty} Y^T(-j\omega)Y(j\omega)\,d\omega$$

Note, finally, that $X(j\omega)$ and $Y(j\omega)$ are ultimately related to the system's frequency response $G(j\omega) = CX(j\omega) + D = Y(j\omega)B + D$.

By definition, the state directions t_i and u_i decompose X and Y into the following outer product sums

$$X = \sum_{i=1}^{n} t_i v_{c_i} t_i^T$$

$$Y = \sum_{i=1}^{n} u_i v_{o_i} u_i^T$$

where v_{c_i} and v_{o_i} are real non-negative scalars and where $u_i^T t_i = 1$ and $u_i^T t_j = 0$ for all $i \neq j$. It is known[6] that the importance of the contribution from state direction t_i to the input-output behavior (i.e., frequency response) system is reflected by the relative magnitude of the product $v_{c_i}v_{o_i}$ where this product is the ith Hankel singular value of $G(s)$, each of which is real, non-negative, and invariant to state-space transformation. The matrix product

$$XY = \sum_{i=1}^{n} t_i v_{c_i} v_{o_i} u_i^T$$

shows that the state directions t_i are eigenvectors of XY and the products $v_{c_i}v_{o_i}$ are the eigenvalues. In other words, state directions t_i most significant to the system's input-output behavior have the larger values for $v_{c_i}v_{o_i}$.

This leads to the so-called internally balanced reduction technique.[6] The reduced-order model is obtained by using the state directions t_i to transform the system to internally balanced states and truncating the least important states, based on the relative size of the eigenvalues $v_{c_i}v_{o_i}$. As noted in Ref. 5, the reduced-order model will inherently lead to a good approximation in the frequency range where the full-order system's frequency response magnitude is large, but this may not be the frequency range of interest (i.e., loop crossover may occur in another frequency range).

› correct this situation, frequency weighting has been in-orated into this approach.[5,7] Consider a weighting filter

$$\dot{x}_w = A_w x_w + B_w \delta$$

$$u = C_w x_w$$

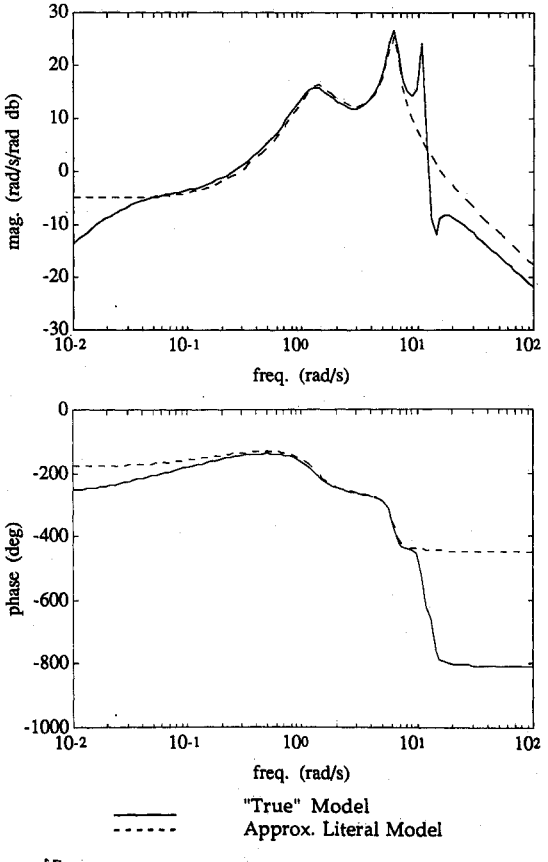

Fig. 4 $G_q^{\delta E}(s)$ **frequency response for the approximate literal model.**

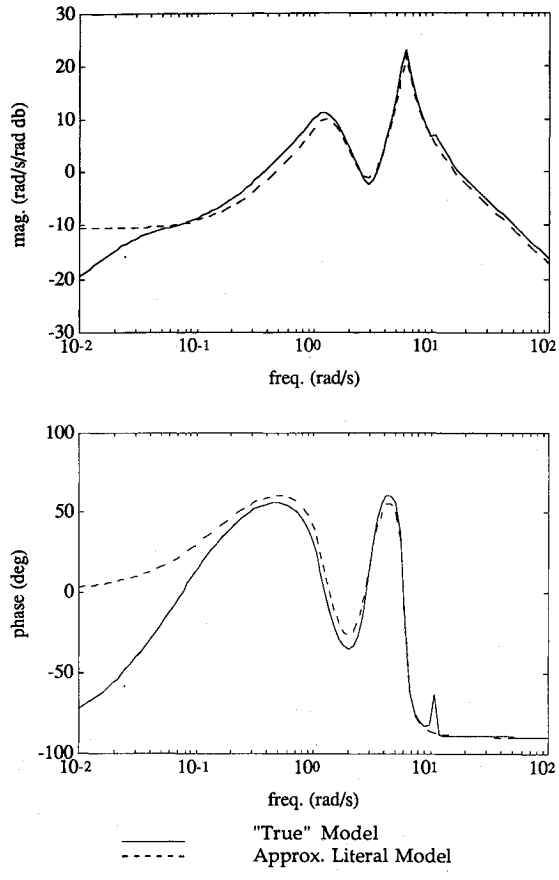

Fig. 5 $G_q^{\delta C}(s)$ frequency response for the approximate literal model.

which is well attenuated outside the frequency range of interest. Let this filter be in cascade with the original system. Decomposing the controllability and observability grammians for the cascaded system leads to frequency-weighted internally balanced states that can readily be reduced by truncation as before. Appendix B from Ref. 5 summarizes this frequency-weighted internally balanced reduction. Note that frequency-weighted internally balanced reduction can only be applied to asymptotically stable systems or asymptotically stable subsystems of a larger system.[5,7]

Truncation

Assume the system is in polynomial matrix form, as in Appendix A, or

$$\begin{bmatrix} A(s) & c(s) \\ r(s) & m(s) \end{bmatrix} \begin{bmatrix} Z(s) \\ z_r(s) \end{bmatrix} = \begin{bmatrix} B(s) \\ b_r(s) \end{bmatrix} U(s) \tag{5}$$

$$Y(s) = M(s)Z(s) + m_r(s)z_r(s) + P(s)U(s)$$

Here $Y(s)$ is the vector of responses, $U(s)$ the vector of inputs, and $[Z^T(s), z_r(s)]^T$ the vector of system degrees of freedom. Assume that $z_r(s)$ is a scalar, and then $m(s)$ is also scalar; $r(s)$ and $b_r(s)$ are row vectors; and $c(s)$ and $m_r(s)$ are column vectors. Define the notation $A_i \mid B_j$ as the matrix formed from the matrix A, but its ith column is replaced by the jth column of B. Then using the properties of the determinant of a partitioned matrix, along with Cramer's rule, yields

$$\frac{Z_i(s)}{U_j(s)} = \frac{m \det[A_i \mid B_j - cm^{-1}(r_i \mid b_{r_j})]}{m \det[A - cm^{-1}r]}$$

$$\frac{z_r(s)}{U_j(s)} = \frac{b_{r_j} \det[A - B_j b_{r_j}^{-1} r]}{m \det[A - cm^{-1}r]}$$

where the (s) denoting functional dependence has been dropped for notational brevity.

Assume now that

$$c_k r_l \ll m; \qquad k,l = 1, \ldots, n \tag{6a}$$

$$B_{j_k} r_l \ll b_{r_j}; \qquad k,l = 1, \ldots, n \tag{6b}$$

$$c_k (r_i \mid b_{r_j})_l \ll m; \qquad k,l = 1, \ldots, n \tag{6c}$$

where dim $[Z(s)] = n$. Then

$$A_i \mid B_j - cm^{-1}(r_i \mid b_{r_j}) \approx A_i \mid B_j$$

$$A - B_j b_{r_j}^{-1} r \approx A$$

$$A - cm^{-1}r \approx A$$

and Z_i and z_r become

$$\frac{Z_i(s)}{U_j(s)} \approx \frac{\hat{Z}_i(s)}{U_j(s)} = \frac{\det[A_i \mid B_j]}{\det[A]} \tag{7a}$$

$$\frac{z_r(s)}{U_j(s)} \approx b_{r_j}/m \tag{7b}$$

Note that $Z_i(s)/U_j(s)$ is simply that obtained if the degree of freedom z_r was truncated from the model (or not included in the modeling from the outset).

Now (consistent with the model in Appendix A), let $m(s) = a_r s^2 + d_r s + k_r$ and $b_{r_j}(s) = b_{r_j}$ (a_r, d_r, k_r, b_{r_j} scalar constants), and consider a high-frequency approximation, or let $|s| \to \infty$, leading to $|b_{r_j}(s)/m(s)| \to 0$. In this case (or if $m_r b_{r_j} \approx 0$ in general), the approximate model is the well-known truncated model

$$Y(s) \approx M(s)\hat{Z}(s) + P(s)U(s)$$

$$\frac{\hat{Z}_i(s)}{U_j(s)} = \frac{\det[A_i \mid B_j]}{\det[A]}$$

This approximation will produce a model with the desired characteristics when assumptions (6) are valid and the crossover frequency is well above $\sqrt{|k_r/a_r|}$ and $\sqrt{|b_{r_j}/a_r|}$.

In the special case with the system transformed into modal coordinates, Eq. (5) becomes

$$\begin{bmatrix} (sI - \Lambda) & 0 \\ 0 & (sI - \Lambda_r) \end{bmatrix} \begin{bmatrix} N(s) \\ N_r(s) \end{bmatrix} = \begin{bmatrix} B \\ B_r \end{bmatrix} U(s)$$

$$Y(s) = MN(s) + M_r N_r(s) + PU(s)$$

with Λ and Λ_r diagonal. Now, assumptions (6) are clearly satisfied. Truncation of the modal coordinates N_r will therefore lead to a good approximation in the frequency range well above the magnitude of the associated eigenvalues (Λ_r). In fact, the transfer-function error resulting from this order reduction is

$$E(s) = G'(s) - G(s) = M_r(sI - \Lambda_r)^{-1} B_r$$

It can be seen that each element of $E(s)$ will be small when $|s| \gg |\Lambda_{rii}|$ and $|s| \gg |(M_r B_r)_{ij}|$.

Residualization

Referring back to Eq. (5), and assuming the same structure for $m(s)$ and $b_{r_j}(s)$, consider now a low-frequency approximation such that $|s| \to 0$, leading to $b_{r_j}(s)/m(s) \to b_{r_j}/k_r$, a

constant scalar. In this case, the approximation is the well-known residualized model

$$Y(s) \approx M(s)\hat{Z}(s) + m_r(s)\sum_{j=1}^{q}(b_{r_j}/k_r)U_j(s) + P(s)U(s)$$

$$\frac{\hat{Z}_i(s)}{U_j(s)} = \frac{\det[A_i \mid B_j]}{\det[A]}$$

where $\dim[U(s)] = q$. This model will have the necessary validity when assumptions (6) are satisfied and crossover frequency is well below $\sqrt{|k_r/a_r|}$.

Again consider the special case where the system is in modal coordinates and then assumptions (6) are clearly satisfied. This residualized-mode model will therefore lead to a good approximation in the frequency range well below the magnitude of the associated eigenvalues (Λ_r). In this case, the transfer-function error is

$$E(s) = M_r(sI - \Lambda_r)^{-1}B_r + M_r(\Lambda_r)^{-1}B_r$$

It can be seen that each element of $E(s)$ will be small when $|s| \ll |\Lambda_{rii}|$.

Approximate Literal Expressions

The transfer-function matrix $G(s)$ for the lower-order model can be computed numerically using the previous methods. Attention will now turn to a simplification technique, related to the technique in Ref. 2, which yields approximate, closed-form literal expressions for the poles and zeros of the system transfer function (matrix).

The method is based on first-order sensitivity theory and can, in principle, be applied to a model of higher order. The basic ideal is to obtain approximations for the factors of a polynomial by approximating the coefficients of the polynomial by the first two terms of a Taylor series. To keep the algebra tractable here, and to explain the method by means of example, consider an already simplified system in polynomial matrix form, as in Appendix C. This particular model may be obtained via reducing the model in Appendix A, by truncating the surge velocity u and residualizing the second through the fourth generalized elastic deflections η_i for the aircraft in Ref. 1.

Consider now the solution for one element of the transfer-function matrix, namely,

$$G_{q^T}^{\delta_E}(s) = \frac{N(s)}{D(s)}$$

Applying Cramer's rule to the model in Appendix C yields

$$\begin{aligned} D(s) = &-\left(\frac{Z_{\dot{\eta}_1}}{V_{T_1}}s + \frac{Z_{\eta_1}}{V_{T_1}}\right)\cdot[M_\alpha F_{1_q}s + F_{1_\alpha}(s^2 - M_q s)] \\ &-(M_{\dot{\eta}_1}s + M_{\eta_1})\cdot\left[F_{1_q}s\left(s - \frac{Z_\alpha}{V_{T_1}}\right) + \left(1 + \frac{Z_q}{V_{T_1}}\right)F_{1_\alpha}s\right] \\ &+\underline{[s^2 + (2\zeta_1\omega_1 - F_{1_{\dot{\eta}_1}})s + (\omega_1^2 - F_{1_{\eta_1}})]} \\ &\times\underline{\left[\left(s - \frac{Z_\alpha}{V_{T_1}}\right)(s^2 - M_q s) - \left(1 + \frac{Z_q}{V_{T_1}}\right)M_\alpha s\right]} \end{aligned} \tag{8a}$$

$$\begin{aligned} N(s) = &\frac{Z_{\delta_E}}{V_{T_1}}\cdot(s\cdot\{M_\alpha[s^2 + (2\zeta_1\omega_1 - F_{1_{\dot{\eta}_1}})s + (\omega_1^2 - F_{1_{\eta_1}})] \\ &+F_{1_\alpha}(M_{\dot{\eta}_1}s + M_{\eta_1})\} - \phi_1' s\cdot[M_\alpha F_{1_q}s + F_{1_\alpha}(s^2 - M_q s)]) \\ &+M_{\delta_E}\cdot\left(s\cdot\underline{\left\{\left(s - \frac{Z_\alpha}{V_{T_1}}\right)[s^2 + (2\zeta_1\omega_1 - F_{1_{\dot{\eta}_1}})s}\right.\right. \\ &\underline{\left.\left.+(\omega_1^2 - F_{1_{\eta_1}})\right] - F_{1_\alpha}\left(\frac{Z_{\dot{\eta}_1}}{V_{T_1}}s + \frac{Z_{\eta_1}}{V_{T_1}}\right)\right\}} \\ &-\phi_1' s\cdot\left[F_{1_q}s\left(s - \frac{Z_\alpha}{V_{T_1}}\right) + \left(1 + \frac{Z_q}{V_{T_1}}\right)F_{1_\alpha}s\right]\Bigg) \\ &+F_{1_{\delta E}}\cdot\left\{s\cdot\left[\left(s - \frac{Z_\alpha}{V_{T_1}}\right)(M_{\dot{\eta}_1}s + M_{\eta_1})\right.\right. \\ &\left.+M_\alpha\left(\frac{Z_{\dot{\eta}_1}}{V_{T_1}}s + \frac{Z_{\eta_1}}{V_{T_1}}\right)\right] - \phi_1' s\cdot\underline{\left[\left(s - \frac{Z_\alpha}{V_{T_1}}\right)(s^2 - M_q s)\right.} \\ &\left.\underline{\left.-M_\alpha\left(1 + \frac{Z_q}{V_{T_1}}\right)s\right]}\right\} \end{aligned} \tag{8b}$$

Also, consider the numerical solution for the same transfer function obtained via any appropriate means, or

$$\begin{aligned} G_{q^T}^{\delta_E}(s) &= \frac{13s(s + 0.23)(s - 3.4)(s + 4.0)}{s(s^2 + 0.88s + 1.6)(s^2 + 1.0s + 36)} \\ &= \frac{K_{q^T}^{\delta_E}s[s + {}_{sp}(1/T)_{q^T}^{\delta_E}][s + {}_{f_{1_1}}(1/T)_{q^T}^{\delta_E}][s + {}_{f_{1_2}}(1/T)_{q^T}^{\delta_E}]}{s[s^2 + (2\zeta\omega)_{sp}s + (\omega^2)_{sp}][s^2 + (2\zeta\omega)_{f_1}s + (\omega^2)_{f_1}]} \\ &= \frac{n_4 s^4 + n_3 s^3 + n_2 s^2 + n_1 s}{s^5 + d_4 s^4 + d_3 s^3 + d_2 s^2 + d_1 s} \end{aligned} \tag{9}$$

One now selects approximate terms, one from $D(s)$ and one from $N(s)$, in Eqs. (8) that best satisfy the following two criteria.

1) The literal expressions for the approximate terms must factor into the same structure as found in the numerical model (poles/zeros). For example, the literal expression for the approximate term for $D(s)$ must have two pairs of complex roots plus one root at the origin, whereas that for $N(s)$ must have four real roots, including one at the origin [see Eq. (9)].

2) The numerical factors calculated from those approximate terms should be as close as possible to the true numerical factors in Eq. (9).

In this example, the approximate terms are selected as the underlined terms in Eqs. (8) yielding

$$\begin{aligned} \tilde{D}(s) &= s\left\{s^2 + \left(-\frac{Z_\alpha}{V_{T_1}} - M_q\right)s + \left[\frac{Z_\alpha}{V_{T_1}}M_q - \left(1 + \frac{Z_q}{V_{T_1}}\right)M_\alpha\right]\right\} \\ &\quad\cdot[s^2 + (2\zeta_1\omega_1 - F_{1_{\dot{\eta}_1}})s + (\omega_1^2 - F_{1_{\eta_1}})] \\ &= s[s^2 + (2\tilde{\zeta}\omega)_{sp}s + (\tilde{\omega}^2)_{sp}][s^2 + (2\tilde{\zeta}\omega)_{f_1}s + (\tilde{\omega}^2)_{f_1}] \\ &= s(s^2 + 1.2s + 3.8)(s^2 + 0.62s + 35) \\ &= s^5 + \tilde{d}_4 s^4 + \tilde{d}_3 s^3 + \tilde{d}_2 s^2 + \tilde{d}_1 s \end{aligned} \tag{10a}$$

and

$$\begin{aligned} \tilde{N}(s) &= (M_{\delta_E} - \phi_1' F_{1_{\delta E}})s\left[s + \left(-\frac{Z_\alpha}{V_{T_1}}\right)\right]\left[s + \left(\frac{b - [b^2 - 4c]^{1/2}}{2}\right)\right] \\ &\quad\times\left[s + \left(\frac{b + [b^2 - 4c]^{1/2}}{2}\right)\right] \\ &= \tilde{K}_{q^T}^{\delta_E}s\,[s + {}_{sp}(1/\tilde{T})_{q^T}^{\delta_E}][s + {}_{f_{1_1}}(1/\tilde{T})_{q^T}^{\delta_E}][s + {}_{f_{1_2}}(1/\tilde{T})_{q^T}^{\delta_E}] \\ &= 13s(s + 0.42)(s - 3.3)(s + 4.2) \\ &= \tilde{n}_4 s^4 + \tilde{n}_3 s^3 + \tilde{n}_2 s^2 + \tilde{n}_1 s \end{aligned} \tag{10b}$$

where

$$b = \frac{(2\zeta_1\omega_1 - F_{1\dot{\eta}_1})M_{\delta_E} + \phi_1' M_q F_{1_{\delta E}}}{M_{\delta_E} - \phi_1' F_{1_{\delta E}}}$$

$$c = \frac{(\omega_1^2 - F_{1\eta_1})M_{\delta_E}}{M_{\delta_E} - \phi_1' F_{1_{\delta E}}}$$

Now, by expanding Eq. (9), one can determine the functional dependence of the polynomial coefficients upon the factors. For example,

$$d_1 = (\omega^2)_{sp}(\omega^2)_{f_1} \tag{11}$$

$$n_1 = K_{q'sp}^{\delta_E}(1/T)_{q'f_{1_1}}^{\delta_E}(1/T)_{q'f_{1_2}}^{\delta_E}(1/T)_{q'}^{\delta_E}$$

Noting this functional dependence, expand each coefficient in a Taylor series where the leading term in the series is taken as the approximate coefficients in Eqs. (10). For example,

$$d_1 = \tilde{d}_1 + \frac{\partial \tilde{d}_1}{\partial x}\Delta x + \cdots \tag{12a}$$

$$n_1 = \tilde{n}_1 + \frac{\partial \tilde{n}_1}{\partial y}\Delta y + \cdots \tag{12b}$$

where

$$\Delta x = [(\omega^2)_{sp} - (\tilde{\omega}^2)_{sp},\ (2\zeta\omega)_{sp} - (2\tilde{\zeta}\omega)_{sp},\ (\omega^2)_{f_1} - (\tilde{\omega}^2)_{f_1},\ (2\zeta\omega)_{f_1} - (2\tilde{\zeta}\omega)_{f_1}]^T$$

$$= [\Delta(\tilde{\omega}^2)_{sp},\ \Delta(2\tilde{\zeta}\omega)_{sp},\ \Delta(\tilde{\omega}^2)_{f_1},\ \Delta(2\tilde{\zeta}\omega)_{f_1}]^T$$

$$\Delta y = [K_{q'}^{\delta_E} - \tilde{K}_{q'}^{\delta_E},\ {}_{sp}(1/T)_{q'}^{\delta_E} - {}_{sp}(1/\tilde{T})_{q'}^{\delta_E},\ {}_{f_{1_1}}(1/T)_{q'}^{\delta_E} - {}_{f_{1_1}}(1/\tilde{T})_{q'}^{\delta_E},\ {}_{f_{1_2}}(1/T)_{q'}^{\delta_E} - {}_{f_{1_2}}(1/\tilde{T})_{q'}^{\delta_E}]^T$$

$$= [\Delta\tilde{K}_{q'}^{\delta_E},\ \Delta_{sp}(1/\tilde{T})_{q'}^{\delta_E},\ \Delta_{f_{1_1}}(1/\tilde{T})_{q'}^{\delta_E},\ \Delta_{f_{1_2}}(1/\tilde{T})_{q'}^{\delta_E}]^T$$

Corrections to the approximate factors (i.e., Δx and Δy) are now sought. Using the Taylor series for each polynomial coefficient such as Eqs. (12) and neglecting higher-order terms, one can solve for Δx and Δy. This calculation requires the literal expressions for $d_i - \tilde{d}_i$ and $n_i - \tilde{n}_i$ obtained from the nonunderlined term in Eq. (8) and the literal expressions for

$$\frac{\partial \tilde{d}_i}{\partial x} \quad \text{and} \quad \frac{\partial \tilde{n}_i}{\partial y}$$

obtained from differentiation of expressions similar to Eq. (11).

The approximate literal model is finally obtained by summing the approximate factors and the corresponding corrections. For example,

$$G_{q'}^{\delta_E}(s) = \frac{N(s)}{D(s)}$$

where

$$D(s) \approx s[s^2 + \{(2\tilde{\zeta}\omega)_{sp} + \Delta(2\tilde{\zeta}\omega)_{sp}\}s + \{(\tilde{\omega}^2)_{sp} + \Delta(\tilde{\omega}^2)_{sp}\}]$$

$$\cdot[s^2 + \{(2\tilde{\zeta}\omega)_{f_1} + \Delta(2\tilde{\zeta}\omega)_{f_1}\}s + \{(\tilde{\omega}^2)_{f_1} + \Delta(\tilde{\omega}^2)_{f_1}\}]$$

and

$$N(s) \approx (\tilde{K}_{q'}^{\delta_E} + \Delta\tilde{K}_{q'}^{\delta_E})s[s + \{{}_{sp}(1/\tilde{T})_{q'}^{\delta_E} + \Delta_{sp}(1/\tilde{T})_{q'}^{\delta_E}\}]$$

$$\cdot[s + \{{}_{f_{1_1}}(1/\tilde{T})_{q'}^{\delta_E} + \Delta_{f_{1_1}}(1/\tilde{T})_{q'}^{\delta_E}\}][s + \{{}_{f_{1_2}}(1/\tilde{T})_{q'}^{\delta_E} + \Delta_{f_{1_2}}(1/\tilde{T})_{q'}^{\delta_E}\}]$$

Example Results

To be obtained now is a reduced order model that is valid in the anticipated crossover frequency range. Assume the control system requirements are such that this range must be 1–10 rad/s. The vehicle discussed previously will be modeled, and the true model is taken as that in Appendix A with four elastic modes. A fourth-order model will be sought based on the observation that the true model has two complex modes in the crossover frequency range.

Two reduced-order models will actually be obtained. One model is obtained by truncating the surge velocity u and pitch angle θ and employing the frequency-weighted internally balanced technique using a bandpass filter with unity magnitude in the 1–10 rad/s frequency range and 40 db/dec magnitude roll off on either side of the pass band. Here, truncation of u was necessary to eliminate an unstable phugoid pole, and truncation of θ was necessary to eliminate the associated pole at the origin. The other reduced-order model (an effective fourth-order model due to a pole/zero cancellation at the origin) is obtained by truncating the surge velocity u (i.e., a short-period approximation) and residualizing the second through the fourth generalized elastic deflections η_i. Appendices D–F contain the transfer functions for the original full-order and the two reduced-order models, and Figs. 2 and 3 show the q'/δ_E and q'/δ_C frequency responses, respectively.

The q'/δ_E and q'/δ_C frequency-response errors [see Eq. (2)] are simply the distances between the Bode magnitudes of the true model and the reduced-order models in Figs. 2 and 3. Observe that the reduced-order models accurately approximate the true model in the 1–10 rad/s frequency range as desired. Similar results are obtained for the other transfer functions in Appendices D–F, in that the reduced-order models are highly accurate in the 1–10 rad/s frequency range, as desired. Specifically, the crossover frequency norm $[\|E(j\omega)\|_{cf}$, see Eq. (3)] is 38 for the truncation/frequency-weighted internally balanced model and 170 for the truncation/residualization model for the model units selected.

Discussion of Results

For control synthesis applications, critical features in the q'/δ_E transfer function, for example, are the nonminimum phase zero located near 3.4 rad/s (see Appendix F and Fig. 2) and the lightly damped complex poles near 6 rad/s (see Appendix F and Fig. 2). These characteristics have been shown[8] to limit the stability robustness of a candidate multivariable control law, based on a literal singular-value analysis. Also, a critical feature in the q'/δ_C transfer function is the dipole structure near 3 and 6 rad/s (see Appendix F and Fig. 3). Recall that nonminimum phase zeros limit the allowable loop gain and yield undesirable initial time-response behavior. Lightly damped complex poles can also limit stability robustness, as well as contribute to undesirable time responses. Dipole structures can also critically affect closed-loop stability.

To expose the physics behind these critical characteristics, an approximate literal model is developed from the truncation/residualization model given in Appendix C. Note that a higher-order model could conceivably be used. As we shall see, however, this is not required here to obtain valid results.

Appendix G lists the approximate literal expressions for the factored transfer functions where the underlined terms were

selected as the approximate terms, and the remaining terms are the corrections. Appendix H also contains the transfer functions obtained from the literal expressions in Appendix G, and Figs. 4 and 5 show the q'/δ_E and q'/δ_C frequency responses, respectively, for this simplified model along with the true model. Observe that the literal model accurately approximates the true model in the 1–10 rad/s frequency range. By comparing similar results for the other transfer functions in Appendices D, F, and H, one observes that the literal approximations are quite accurate.

Now to expose the parameters affecting the nonminimum phase zero in the q'/δ_E transfer function (see Appendix F), consider the expression for ${}_{f_1}(1/T)_{q'}^{\delta_E}$ appearing in Appendix G, or

$$ {}_{f_1}\left(\frac{1}{T}\right)_{q'}^{\delta_E} \approx \frac{b - [b^2 - 4c]^{1/2}}{2} + \frac{F_{1_q} M_{\delta_E}}{2F_{1_{\delta E}}} $$

$$ = -3.3 + (-0.23) \tag{13} $$

with the following numerical values:

$$ M_q = -0.830\ 1/\text{s}, \quad M_{\delta_E} = -5.12\ 1/\text{s}^2, \quad F_{1_q} = -78.4\ 1/\text{s} $$

$$ F_{1_{\delta E}} = -866\ 1/\text{s}^2, \quad (\omega_1^2 - F_{1_{\eta_1}}) = 34.8\ 1/\text{s}^2 $$

$$ (2\zeta_1\omega_1 - F_{1_{\dot\eta_1}}) = 0.621\ 1/\text{s}, \quad \phi_1'(x) = 0.0210\ \text{ft/ft} $$

$$ b = 0.912\ 1/\text{s}, \quad c = -13.6\ 1/\text{s}^2 $$

As seen from Eq. (13), the zero location is primarily a function of the first term $(b - [b^2 - 4c]^{1/2})/2$, which in turn is primarily a function of the parameter c as given in Appendix G, or

$$ c = \frac{(\omega_1^2 - F_{1_{\eta_1}}) M_{\delta_E}}{M_{\delta_E} - \phi_1'(x) F_{1_{\delta E}}} \tag{14} $$

Evidently, the key parameters are the elevator control derivatives M_{δ_E} and $F_{1_{\delta E}}$, elastic mode structural frequency and aerodynamic stiffness $(\omega_1^2 - F_{1_{\eta_1}})$, and the elastic mode slope $\phi_1'(x)$. From the denominator in Eq. (14), it is apparent that the nonminimum phase characteristic is directly related to the control power affecting the rigid-body and elastic pitch motions (i.e., up elevator induces rigid-body pitch up and elastic pitch down). Further, it can be seen how the pitch-rate sensor location, through $\phi_1'(x)$, and the aeroelastic mode frequency $(\omega_1^2 - F_{1_{\eta_1}})$ affect the nonminimum phase characteristics.

Attention is now turned to the lightly damped complex poles in the q'/δ_E transfer function (see Appendix F). The expression for the damping term $(2\zeta\omega)_{f_1}$ appearing in Appendix G is

$$ (2\zeta\omega)_{f_1} \approx (2\zeta_1\omega_1 - F_{1_{\dot\eta_1}}) + \frac{M_{\eta_1} F_{1_q} + \{(Z_{\eta_1}/V_{T_1}) + [1 + (Z_q/V_{T_1})] M_{\dot\eta_1}\} F_{1_\alpha}}{(\omega_1^2 - F_{1_{\eta_1}})} $$

$$ = 0.62 + 0.35 \tag{15} $$

with the following numerical values:

$$ \left(1 + \frac{Z_q}{V_{T_1}}\right) = 1.03, \quad \frac{Z_{\eta_1}}{V_{T_1}} = -0.00267\ 1/\text{s} $$

$$ M_{\eta_1} = -0.0655\ 1/\text{s}^2 \quad M_{\dot\eta_1} = -0.00390\ 1/\text{s} $$

$$ F_{1_\alpha} = -1040\ 1/\text{s}^2, \quad F_{1_q} = -78.4\ 1/\text{s} $$

$$ (\omega_1^2 - F_{1_{\eta_1}}) = 34.8\ 1/\text{s}^2, \quad (2\zeta_1\omega_1 - F_{1_{\dot\eta_1}}) = 0.621\ 1/\text{s} $$

As seen from Eq. (15), the low damping is primarily due to the low elastic mode structural and aerodynamic damping $(2\zeta_1\omega_1 - F_{1_{\dot\eta_1}})$. However, note that approximately one-third of the total damping originates from other sources, such as aerodynamic coupling between the rigid and elastic degrees of freedom, i.e.,

$$ M_{\eta_1} F_{1_q}, \quad \frac{Z_{\eta_1}}{V_{T_1}} F_{1_\alpha}, \quad \left(1 + \frac{Z_q}{V_{T_1}}\right) M_{\dot\eta_1} F_{1_\alpha} $$

Finally, consider the dipole structure in the q'/δ_C transfer function (see Appendix F). The dipole consists of the lightly damped complex poles $[s^2 + (2\zeta\omega)_{f_1} s + (\omega^2)_{f_1}]$ and lightly damped complex zeros $[s^2 + {}_{f_1}(2\zeta\omega)_{q'}^{\delta_C} s + {}_{f_1}(\omega^2)_{q'}^{\delta_C}]$. The relative location of the pole and zero along the $j\omega$ axis is determined primarily by the difference between the natural frequency terms $(\omega^2)_{f_1}$ and ${}_{f_1}(\omega^2)_{q'}^{\delta_C}$ appearing in Appendix G, or

$$ (\omega^2)_{f_1} - {}_{f_1}(\omega^2)_{q'}^{\delta_C} \approx (\omega_1^2 - F_{1_{\eta_1}}) + \frac{[1 + (Z_q/V_{T_1})] M_{\eta_1} F_{1_\alpha}}{(\omega_1^2 - F_{1_{\eta_1}})} $$

$$ - \left\{ \frac{(\omega_1^2 - F_{1_{\eta_1}}) M_{\delta_C}}{M_{\delta_C} - \phi_1'(x) F_{1_{\delta C}}} - \frac{M_{\eta_1} + \phi_1'(x)[1 + (Z_q/V_{T_1})] M_\alpha}{\phi_1'(x)} \right\} $$

$$ = 35 + 2.0 - \{2.0 - (-6.5)\} \tag{16} $$

with the following numerical values:

$$ \left(1 + \frac{Z_q}{V_{T_1}}\right) = 1.03, \quad M_\alpha = -3.33\ 1/\text{s}^2 $$

$$ M_{\eta_1} = -0.0655\ 1/\text{s}^2, \quad M_{\delta_C} = 0.809\ 1/\text{s}^2 $$

$$ F_{1_\alpha} = -1040\ 1/\text{s}^2, \quad F_{1_{\delta C}} = -631\ 1/\text{s}^2 $$

$$ (\omega_1^2 - F_{1_{\eta_1}}) = 34.8\ 1/\text{s}^2, \quad \phi_1'(x) = 0.0210\ \text{ft/ft} $$

As seen from Eq. (16), the second and third terms approximately cancel, leaving the dipole structure primarily a function of the elastic mode structural frequency and aerodynamic stiffness $(\omega_1^2 - F_{1_{\eta_1}})$, stability derivatives (Z_q/V_{T_1}), M_α, and M_{η_1}, and the elastic mode slope $\phi_1'(x)$. For fixed stability derivatives (Z_q/V_{T_1}), M_α, and M_{η_1}, it is apparent the pole location is directly related to the elastic mode structural frequency and aerodynamic stiffness, whereas the zero location is directly related to the q' sensor location through the elastic mode slope.

Conclusions

The importance of a dynamic model's validity in the (multivariable) region of crossover was underscored, and three model simplification techniques capable of delivering valid models (in this sense) were presented. Classical truncation and residualization were shown to be capable of yielding a good low-order model, but a newer numerical procedure known as the frequency-weighted balanced technique led to superior results in this case.

A literal simplified model was also shown to yield excellent results, and the procedure was presented herein. This approach, furthermore, was shown to lead to closed-form analytical expression for the key dynamic characteristics and, hence, expose the fundamental causes for these characteristics.

Appendix A: Elastic Aircraft Longitudinal Dynamic and Response Equations in Polynomial Matrix Form

$$
\begin{bmatrix}
s-X_u & -X_\alpha & -X_q s - X_\theta & -X_{\dot\eta_1}s - X_{\eta_1} & -X_{\dot\eta_2}s - X_{\eta_2} & \cdots & 0 & 0 \\
-\frac{Z_u}{V_{T_1}} & s-\frac{Z_\alpha}{V_{T_1}} & -\left(1+\frac{Z_q}{V_{T_1}}\right)s & -\frac{Z_{\dot\eta_1}}{V_{T_1}}s-\frac{Z_{\eta_1}}{V_{T_1}} & -\frac{Z_{\dot\eta_2}}{V_{T_1}}s-\frac{Z_{\eta_2}}{V_{T_1}} & & 0 & 0 \\
-M_u & -M_\alpha & s^2-M_q s & -M_{\dot\eta_1}s-M_{\eta_1} & -M_{\dot\eta_2}s-M_{\eta_2} & & 0 & 0 \\
-F_{1_u} & -F_{1_\alpha} & -F_{1_q}s & s^2+(2\zeta_1\omega_1-F_{1_{\dot\eta_1}})s+(\omega_1^2-F_{1_{\eta_1}}) & -F_{1_{\dot\eta_2}}s-F_{1_{\eta_2}} & & 0 & 0 \\
-F_{2_u} & -F_{2_\alpha} & -F_{2_q}s & -F_{2_{\dot\eta_1}}s-F_{2_{\eta_1}} & s^2+(2\zeta_2\omega_2-F_{2_{\dot\eta_2}})s+(\omega_2^2-F_{2_{\eta_2}}) & & 0 & 0 \\
\vdots & & & & & & \vdots & \vdots \\
-K_u & -K_\alpha & -K_q s & -K_{\dot\eta_1}s-K_{\eta_1} & -K_{\dot\eta_2}s-K_{\eta_2} & & 1 & 0 \\
0 & 0 & -s & \phi_1'(x)s & \phi_2'(x)s & \cdots & 0 & 1
\end{bmatrix}
\begin{bmatrix} u(s) \\ \alpha(s) \\ \theta(s) \\ \eta_1(s) \\ \eta_2(s) \\ \vdots \\ a_z'(s) \\ q'(s) \end{bmatrix}
=
\begin{bmatrix}
X_{\delta_E} & X_{\delta_C} \\
\frac{Z_{\delta_E}}{V_{T_1}} & \frac{Z_{\delta_C}}{V_{T_1}} \\
M_{\delta_E} & M_{\delta_C} \\
F_{1_{\delta E}} & F_{1_{\delta C}} \\
F_{2_{\delta E}} & F_{2_{\delta C}} \\
\vdots & \vdots \\
K_{\delta_E} & K_{\delta_C} \\
0 & 0
\end{bmatrix}
\begin{bmatrix} \delta_E(s) \\ \delta_C(s) \end{bmatrix}
$$

$$K_u = Z_u - xM_u + \sum_i \phi_i(x)F_{i_u}, \quad K_{\eta_i} = Z_{\eta_i} - xM_{\eta_i} - \phi_i(x)(\omega_1^2 - F_{i_{\eta_i}}) + \sum_{j,j\neq i} \phi_j(x)F_{j_{\eta_i}}, \quad K_{\delta_E} = Z_{\delta_E} - xM_{\delta_E} + \sum_i \phi_i(x)F_{i_{\delta E}}$$

$$K_\alpha = Z_\alpha - xM_\alpha + \sum_i \phi_i(x)F_{i_\alpha}, \quad K_{\dot\eta_i} = Z_{\dot\eta_i} - xM_{\dot\eta_i} - \phi_i(x)(2\zeta_i\omega_i - F_{i_{\dot\eta_i}}) + \sum_{j,j\neq i} \phi_j(x)F_{j_{\dot\eta_i}}, \quad K_{\delta_C} = Z_{\delta_C} - xM_{\delta_C} + \sum_i \phi_i(x)F_{i_{\delta C}}$$

$$K_q = Z_q - xM_q + \sum_i \phi_i(x)F_{i_q}$$

Appendix B: Frequency-Weighted Internally Balanced Reduction

Given: System state-space description A, B, C, D and weighting filter state-space description A_w, B_w, C_w

Find: rth order system

Step 1: Solve for X and Y from

$$\begin{bmatrix} A & BC_w \\ 0 & A_w \end{bmatrix}\begin{bmatrix} X & X_{12} \\ X_{21} & X_{22} \end{bmatrix} + \begin{bmatrix} X & X_{12} \\ X_{21} & X_{22} \end{bmatrix}\begin{bmatrix} A^T & 0 \\ C_w^T B^T & A_w^T \end{bmatrix} + \begin{bmatrix} 0 & 0 \\ 0 & B_w B_w^T \end{bmatrix} = 0$$

$$A^T Y + YA + C^T C = 0$$

Step 2: Find T and Σ where $XY = T\Sigma^2 T^{-1}$, $T = [T_r, T_{n-r}]$, $T^{-T} = [U_r, U_{n-r}]$

$$\Sigma^2 = \begin{bmatrix} \Sigma_r^2 & 0 \\ 0 & \Sigma_{n-r}^2 \end{bmatrix}$$

$$\Sigma_r^2 = \text{diag}(v_{c_i}v_{o_i}); \qquad i = 1, \ldots, r$$

$$\Sigma_{n-r}^2 = \text{diag}(v_{c_i}v_{o_i}); \qquad i = r+1, \ldots, n$$

$$v_{c_1}v_{o_1} \geq \cdots \geq v_{c_n}v_{o_n} \geq 0$$

Step 3: r th order system is

$$A_r = U_r^T A T_r, \quad B_r = U_r^T B, \quad C_r = CT_r, \quad D_r = D$$

Appendix C: Elastic Aircraft Longitudinal Dynamic and Response Equations in Polynomial Matrix Form

$$
\begin{bmatrix}
s-\frac{Z_\alpha}{V_{T_1}} & -\left(1+\frac{Z_q}{V_{T_1}}\right)s & -\frac{Z_{\dot\eta_1}}{V_{T_1}}s-\frac{Z_{\eta_1}}{V_{T_1}} & 0 & 0 \\
-M_\alpha & s^2-M_q s & -M_{\dot\eta_1}s-M_{\eta_1} & 0 & 0 \\
-F_{1_\alpha} & -F_{1_q}s & s^2+(2\zeta_1\omega_1-F_{1_{\dot\eta_1}})s+(\omega_1^2-F_{1_{\eta_1}}) & 0 & 0 \\
-K_\alpha & -K_q s & -K_{\dot\eta_1}s-K_{\eta_1} & 1 & 0 \\
0 & -s & \phi_1'(x)s & 0 & 1
\end{bmatrix}
\begin{bmatrix} \alpha(s) \\ \theta(s) \\ \eta_1(s) \\ a_z'(s) \\ q'(s) \end{bmatrix}
=
\begin{bmatrix}
\frac{Z_{\delta_E}}{V_{T_1}} & \frac{Z_{\delta_C}}{V_{T_1}} \\
M_{\delta_E} & M_{\delta_C} \\
F_{1_{\delta E}} & F_{1_{\delta C}} \\
K_{\delta_E} & K_{\delta_C} \\
0 & 0
\end{bmatrix}
\begin{bmatrix} \delta_E(s) \\ \delta_C(s) \end{bmatrix}
$$

Appendix D: Transfer Functions for the True Model

$$G_{a_z'}^{\delta_E}(s) = 52s(s+0.0089)(s+0.020 \pm j1.7)(s+0.36 \pm j11)(s+1.0 \pm j11)(s-1.5 \pm j12)(s+3.1 \pm j14)/D(s) \text{ (ft/s}^2\text{/rad)}$$

$$G_{q'}^{\delta_E}(s) = 8.0s(s+0.051)(s+0.20)(s-3.6)(s+4.0)(s+0.36 \pm j11)(s+2.8 \pm j13)(s-0.57 \pm j13)/D(s) \text{ (rad/s/rad)}$$

$$G_{a_z'}^{\delta_C}(s) = -240s(s+0.0081)(s-0.17 \pm j1.8)(s+0.90 \pm j4.1)(s+0.23 \pm j11)(s+0.36 \pm j11)(s+2.6 \pm j13)/D(s) \text{ (ft/s}^2\text{/rad)}$$

$$G_{q'}^{\delta_C}(s) = 16s(s+0.055)(s+0.12)(s+0.60 \pm j2.9)(s+0.26 \pm j11)(s+0.36 \pm j11)(s+2.6 \pm j13)/D(s) \text{ (rad/s/rad)}$$

where

$$D(s) = (s - 0.033)(s + 0.043)(s + 0.45 \pm j1.2)(s + 0.44 \pm j6.0)(s + 0.22 \pm j11)(s + 0.36 \pm j11)(s + 2.6 \pm j13)$$

Appendix E: Transfer Functions for the Truncated Frequency-Weighted Internally Balanced Model

$$G_{a_z}^{\delta E}(s) = 52(s + 0.020 \pm j1.7)(s - 1.2 \pm j14)/D(s) \text{ (ft/s}^2\text{/rad)}$$

$$G_{q'}^{\delta E}(s) = 15(s + 0.088)(s - 2.9)(s + 3.9)/D(s) \text{ (rad/s/rad)}$$

$$G_{a_z}^{\delta C}(s) = -240(s - 0.18 \pm j1.8)(s + 0.92 \pm j4.1)/D(s) \text{ (ft/s}^2\text{/rad)}$$

$$G_{q'}^{\delta C}(s) = 15(s + 0.090)(s + 0.70 \pm j2.9)/D(s) \text{ (rad/s/rad)}$$

where

$$D(s) = (s + 0.46 \pm j1.2)(s + 0.44 \pm j6.0)$$

Appendix F: Transfer Functions for the Truncated/Residualization Model

$$G_{a_z}^{\delta E}(s) = 46s(s + 0.014 \pm j1.7)(s - 1.7 \pm j14)/D(s) \text{ (ft/s}^2\text{/rad)}$$

$$G_{q'}^{\delta E}(s) = 13s(s + 0.23)(s - 3.4)(s + 4.0)/D(s) \text{ (rad/s/rad)}$$

$$G_{a_z}^{\delta C}(s) = -240s(s - 0.17 \pm j1.8)(s + 1.0 \pm j4.2)/D(s) \text{ (ft/s}^2\text{/rad)}$$

$$G_{q'}^{\delta C}(s) = 14s(s + 0.16)(s + 0.66 \pm j3.0)/D(s) \text{ (rad/s/rad)}$$

where

$$D(s) = s(s + 0.44 \pm j1.2)(s + 0.50 \pm j6.0)$$

Appendix G: Approximate Literal Expressions for the Factored Transfer Functions

$$G_{a_z}^{\delta E}(s) = \frac{K_{a_z}^{\delta E} s[s^2 + {}_{sp}(2\zeta\omega)_{a_z}^{\delta E} s + {}_{sp}(\omega^2)_{a_z}^{\delta E}][s^2 + {}_{f_1}(2\zeta\omega)_{a_z}^{\delta E} s + {}_{f_1}(\omega^2)_{a_z}^{\delta E}]}{D(s)}$$

$$G_{a_z}^{\delta C}(s) = \frac{K_{a_z}^{\delta C} s[s^2 + {}_{sp}(2\zeta\omega)_{a_z}^{\delta C} s + {}_{sp}(\omega^2)_{a_z}^{\delta C}][s^2 + {}_{f_1}(2\zeta\omega)_{a_z}^{\delta C} s + {}_{f_1}(\omega^2)_{a_z}^{\delta C}]}{D(s)}$$

$$G_{q'}^{\delta E}(s) = \frac{K_{q'}^{\delta E} s[s + {}_{sp}(1/T)_{q'}^{\delta E}][s + {}_{f_{1_1}}(1/T)_{q'}^{\delta E}][s + {}_{f_{1_2}}(1/T)_{q'}^{\delta E}]}{D(s)}$$

$$G_{q'}^{\delta C}(s) = \frac{K_{q'}^{\delta C} s[s + {}_{sp}(1/T)_{q'}^{\delta C}][s + {}_{f_1}(2\zeta\omega)_{q'}^{\delta C} s + {}_{f_1}(\omega^2)_{q'}^{\delta C}]}{D(s)}$$

where

$$D(s) = s[s^2 + (2\zeta\omega)_{sp} s + (\omega^2)_{sp}][s^2 + (2\zeta\omega)_{f_1} s + (\omega^2)_{f_1}]$$

and

$$(\omega^2)_{sp} \approx \underline{\frac{Z_\alpha}{V_{T_1}} M_q - \left(1 + \frac{Z_q}{V_{T_1}}\right) M_\alpha} - \frac{[1 + (Z_q/V_{T_1})]M_{\eta_1} F_{1_\alpha}}{(\omega_1^2 - F_{1\eta_1})}$$

$$(2\zeta\omega)_{sp} \approx \underline{-\frac{Z_\alpha}{V_{T_1}} - M_q} - \frac{\{(Z_{\eta_1}/V_{T_1}) + [1 + (Z_q/V_{T_1})]M_{\dot{\eta}_1}\}F_{1_\alpha} + M_{\eta_1} F_{1_q}}{(\omega_1^2 - F_{1\eta_1})}$$

$$K_{a_z}^{\delta E} \approx \underline{K_{\delta_E}}$$

$${}_{sp}(\omega^2)_{a_z}^{\delta E} \approx \underline{\frac{Z_\alpha}{V_{T_1}} M_q} + \frac{[(\omega_1^2 - F_{1\eta_1})K_\alpha + F_{1_\alpha} K\eta_1][1 + (Z_q/V_{T_1})]M_{\delta_E}}{K_{\eta_1} F_{1_{\delta E}}}$$

$${}_{sp}(2\zeta\omega)_{a_z}^{\delta E} \approx \underline{-\frac{Z_\alpha}{V_{T_1}} - M_q} + \frac{[(\omega_1^2 - F_{1\eta_1})M_{\delta_E} + M_{\eta_1} F_{1_{\delta E}}]K_q}{K_{\eta_1} F_{1_{\delta E}}}$$

$${}_{f_1}(\omega^2)_{a_z}^{\delta E} \approx \underline{(\omega_1^2 - F_{1\eta_1}) + \frac{K_{\eta_1} F_{1_{\delta E}}}{K_{\delta_E}}} + \frac{[1 + (Z_q/V_{T_1})]K_\alpha M_{\delta_E}}{K_{\delta_E}}$$

$${}_{f_1}(2\zeta\omega)_{a_z}^{\delta E} \approx \underline{(2\zeta_1\omega_1 - F_{1\dot{\eta}_1}) + \frac{K_{\dot{\eta}_1} F_{1_{\delta E}}}{K_{\delta_E}}} + \frac{[-(\omega_1^2 - F_{1\eta_1})K_{\delta_E} + K_{\eta_1} F_{1_{\delta E}}]K_q M_{\delta_E}}{K_{\eta_1} K_{\delta_E} F_{1_{\delta E}}}$$

$$K_{q'}^{\delta E} \approx \underline{M_{\delta_E} - \phi_1'(x) F_{1_{\delta E}}}$$

$${}_{sp}(1/T)_{q'}^{\delta E} \approx \underline{-\frac{Z_\alpha}{V_{T_1}}} - \frac{(Z_{\eta_1}/V_{T_1})F_{1_\alpha} M_{\delta_E} + (Z_\alpha/V_{T_1})M_{\eta_1} F_{1_{\delta E}}}{(\omega_1^2 - F_{1\eta_1})M_{\delta_E}}$$

$$f_{1_1}(1/T)_q^{\delta_E} \approx \frac{b - [b^2 - 4c]^{1/2}}{2} + \frac{F_{1_q} M_{\delta_E}}{2F_{1_{\delta E}}}$$

$$f_{1_2}(1/T)_q^{\delta_E} \approx \frac{b + [b^2 - 4c]^{1/2}}{2} + \frac{F_{1_q} M_{\delta_E}}{2F_{1_{\delta E}}}$$

$$b = \frac{(2\zeta_1\omega_1 - F_{1_{\dot{\eta}_1}})M_{\delta_E} + \phi_1'(x)M_q F_{1_{\delta E}}}{M_{\delta_E} - \phi_1'(x)F_{1_{\delta E}}}$$

$$(\omega^2)_{f_1} \approx \underline{(\omega_1^2 - F_{1_{\eta_1}})} + \frac{[1 + (Z_q/V_{T_1})]M_{\eta_1}F_{1_\alpha}}{(\omega_1^2 - F_{1_{\eta_1}})}$$

$$(2\zeta\omega)_{f_1} \approx \underline{(2\zeta_1\omega_1 - F_{1_{\dot{\eta}_1}})} + \frac{\{(Z_{\eta_1}/V_{T_1}) + [1 + (Z_q/V_{T_1})]M_{\dot{\eta}_1}\}F_{1_\alpha} + M_{\eta_1}F_{1_q}}{(\omega_1^2 - F_{1_{\eta_1}})}$$

$$K_{a_z'}^{\delta_C} \approx \underline{K_{\delta_C}}$$

$$_{sp}(\omega^2)_{a_z'}^{\delta_C} \approx \underline{\frac{Z_\alpha}{V_{T_1}} M_q} - \frac{[(\omega_1^2 - F_{1_{\eta_1}})K_\alpha + M_{\eta_1}F_{1_\alpha}][1 + (Z_q/V_{T_1})]K_{\delta_C}}{(\omega_1^2 - F_{1_{\eta_1}})K_{\delta_C} + K_{\eta_1}F_{1_{\delta C}}}$$

$$_{sp}(2\zeta\omega)_{a_z'}^{\delta_C} \approx \underline{-\frac{Z_\alpha}{V_{T_1}} - M_q} + \frac{[(\omega_1^2 - F_{1_{\eta_1}})M_{\delta_C} + M_{\eta_1}F_{1_{\delta C}}]K_q - \{M_{\eta_1}F_{1_q} + [1 + (Z_q/V_{T_1})]M_{\dot{\eta}_1}F_{1_\alpha}\}K_{\delta_C}}{(\omega_1^2 - F_{1_{\eta_1}})K_{\delta_C} + K_{\eta_1}F_{1_{\delta C}}}$$

$$_{f_1}(\omega^2)_{a_z'}^{\delta_C} \approx \underline{(\omega_1^2 - F_{1_{\eta_1}}) + \frac{K_{\eta_1}F_{1_{\delta C}}}{K_{\delta_C}}} + \frac{[M_{\eta_1}F_{1_\alpha}K_{\delta_C} - M_\alpha K_{\eta_1}F_{1_{\delta C}}][1 + (Z_q/V_{T_1})]}{(\omega_1^2 - F_{1_{\eta_1}})K_{\delta_C} + K_{\eta_1}F_{1_{\delta C}}}$$

$$_{f_1}(2\zeta\omega)_{a_z'}^{\delta_C} \approx \underline{(2\zeta_1\omega_1 - F_{1_{\dot{\eta}_1}}) + \frac{K_{\dot{\eta}_1}F_{1_{\delta C}}}{K_{\delta_C}}} + \frac{[(Z_\alpha/V_{T_1}) + M_q][1 + (Z_q/V_{T_1})]M_\alpha K_{\delta_C} - M_{\eta_1}K_q F_{1_{\delta C}}}{(\omega_1^2 - F_{1_{\eta_1}})K_{\delta_C} + K_{\eta_1}F_{1_{\delta C}}}$$

$$K_{q'}^{\delta_C} \approx \underline{M_{\delta_C} - \phi_1'(x)F_{1_{\delta C}}}$$

$$_{sp}(1/T)_{q'}^{\delta_C} \approx \underline{-\frac{Z_\alpha}{V_{T_1}}} + \frac{\{\phi_1'(x)[1 + (Z_q/V_{T_1})](Z_\alpha/V_{T_1})M_\alpha + (Z_{\eta_1}/V_{T_1})M_\alpha - (Z_\alpha/V_{T_1})M_{\eta_1}\}F_{1_{\delta C}}}{(\omega_1^2 - F_{1_{\eta_1}})M_{\delta_C}}$$

$$_{f_1}(\omega^2)_{q'}^{\delta_C} \approx \underline{\frac{(\omega_1^2 - F_{1_{\eta_1}})M_{\delta_C}}{M_{\delta_C} - \phi_1'(x)F_{1_{\delta C}}}} - \frac{M_{\eta_1} + \phi_1'(x)[1 + (Z_q/V_{T_1})]M_\alpha}{\phi_1'(x)}$$

$$_{f_1}(2\zeta\omega)_{q'}^{\delta_C} \approx \underline{\frac{(2\zeta_1\omega_1 - F_{1_{\dot{\eta}_1}})M_{\delta_C} + \phi_1'(x)M_q F_{1_{\delta C}}}{M_{\delta_C} - \phi_1'(x)F_{1_{\delta C}}}} - \frac{\phi_1'(x)[1 + (Z_q/V_{T_1})](Z_\alpha/V_{T_1})M_\alpha F_{1_{\delta C}}}{(\omega_1^2 - F_{1_{\eta_1}})M_{\delta_C}}$$

$$c = \frac{(\omega_1^2 - F_{1_{\eta_1}})M_{\delta_E}}{M_{\delta_E} - \phi_1'(x)F_{1_{\delta E}}}$$

Appendix H: Transfer Functions for the Approximate Literal Model

$$G_{a_z'}^{\delta_E}(s) = 46s(s + 0.13 \pm j2.0)(s - 1.9 \pm j14)/D(s) \text{ (ft/s}^2\text{/rad)}$$

$$G_{q'}^{\delta_E}(s) = 13s(s + 0.20)(s - 3.5)(s + 3.9)/D(s) \text{ (rad/s/rad)}$$

$$G_{a_z'}^{\delta_C}(s) = -240s(s - 0.11 \pm j1.8)(s + 0.72 \pm j4.0)/D(s) \text{ (ft/s}^2\text{/rad)}$$

$$G_{q'}^{\delta_C}(s) = 14s(s + 0.16)(s + 0.74 \pm j2.8)/D(s) \text{ (rad/s/rad)}$$

where

$$D(s) = s(s + 0.45 \pm j1.2)(s + 0.48 \pm j6.0)$$

Acknowledgments

This research was supported by NASA Langley Research Center under Grant NAG1-758. Doug Arbuckle was technical monitor. This support is appreciated.

References

[1]Waszak, M. R., and Schmidt, D. K., "Flight Dynamics of Aeroelastic Vehicles," *Journal of Aircraft*, Vol. 25, No. 6, 1988, pp. 563-571.

[2]Pearce, B. F., Johnson, W. A., and Siskind, R. K., "Analytical Study of Approximate Longitudinal Transfer Functions for a Flexible Airframe," ASD-TDR-62-279, Wright-Patterson AFB, OH, June 1962.

[3]Doyle, J. C., and Stein, G., "Multivariable Feedback Design: Concepts for a Classical/Modern Synthesis," *IEEE Transactions on Automatic Control,* Vol. AC-26, No. 1, Feb. 1981, pp. 4–16.

[4]Bacon, B. J., and Schmidt, D. K., "A Fundamental Approach to Equivalent Systems Analysis," *Journal of Guidance, Control, and Dynamics,* Vol. 11, No. 6, 1988, pp. 527–534.

[5]Bacon, B. J., and Schmidt, D. K., "Multivariable Frequency-Weighted Order Reduction," *Journal of Guidance, Control, and Dynamics,* Vol. 12, No. 1, 1989, pp. 97–107.

[6]Moore, B. C., "Principal Component Analysis in Linear Systems: Controllability, Observability, and Model Reduction," *IEEE Transactions on Automatic Control,* Vol. AC-26, No. 1, Feb. 1981, pp. 17–32.

[7]Enns, D. F., "Model Reduction for Control System Design," Ph.D. Dissertation, Dept. of Aeronautics and Astronautics, Stanford Univ., Stanford, CA, June 1984.

[8]Schmidt, D. K., and Newman, B., "Multivariable Flight Control Synthesis and Literal Robustness Analysis for an Aeroelastic Vehicle," AIAA Paper 90-3446, Guidance, Navigation, and Control Conference, Portland, OR, Aug. 1990.